PHYSOR 2002, Seoul, Korea, October 7-10, 2002

RESPONSE MATRIX SOLUTION USING BOUNDARY CONDITION PERTURBATION THEORY FOR THE DIFFUSION APPROXIMATION

Michael Scott McKinley
University of California
Lawrence Livermore National Laboratory
Livermore, CA 94550
mckinley9@llnl.gov

Farzad Rahnema
Georgia Institute of Technology
Nuclear Engineering and Health Physics Programs
The George W. Woodruff School of Mechanical Engineering
Atlanta, GA 30332-0405 USA
farzad.rahnema@me.gatech.edu

ABSTRACT

A second-order response matrix method is developed for solving the diffusion equation in a coarse-mesh grid. In this method, the problem domain is divided into a grid of coarse meshes (nodes) of the size of a fuel assembly. Then, by using the fact that all nodes have the same eigenvalue, an equation is developed for the node interface current to flux ratio. The fine-mesh solution in the domain is then obtained by evaluating perturbation expressions for the core eigenvalue and the flux with the node interface current to flux ratios and the precomputed Green's functions for the unique assemblies in the system. The Green's functions and the perturbation expressions for the eigenvalue and flux are based on a high-order boundary condition perturbation method developed recently. Two example problems are used to assess the accuracy of the new method.

1. INTRODUCTION

Many tools in nuclear design and monitoring make use of nodal methods that assume cross sections are uniform in each node of the size of a fuel assembly in the radial direction. These cross sections are obtained by a homogenization method known as generalized equivalence theory (GET). In practice, the homogenization is performed using single assembly calculations with a zero-current (or a full specular reflective) boundary condition. For highly heterogeneous fuel assemblies and core configurations, the assumption of no net neutron leakage (zero-current) at the assembly interface leads to errors in the homogenized parameters. This is known as the core environmental effect. In reference [1], a high-order boundary condition perturbation method was developed to correct the homogenized cross sections and discontinuity factors for this effect. This method was subsequently applied within the context of GET to improve the accuracy of nodal methods in reference [2]. This high-order method corrects the homogenized parameters within the nodal calculations without any iteration with assembly calculations to achieve nodal and reconstructed fine-

mesh flux and fuel pin power results with arbitrary accuracy in one-dimensional benchmark problems.

Instead of correcting homogenized parameters as in reference [2], in the present work, a response matrix method is developed to first solve for the interface (nodal boundary) condition. Using the interface conditions in the expressions for the core eigenvalue and the fine-mesh flux developed in reference [2], the fine-mesh solution may be determined to an arbitrary accuracy (perturbation order) in the core. We note that this method does not require homogenization of the cross sections and that the response matrix for each unique fuel assembly is precomputed. The response matrix in this case is a Green's function for a fixed source adjoint problem resulting from the high-order boundary condition perturbation method.

2. DERIVATION

Before we can analyze a core configuration, we must first determine the complete initial (unperturbed) solution for each unique assembly in the core. For this paper, the unperturbed state of an assembly will be that of an infinite medium approximation in which the current is zero across the boundary. This is generally known as the single assembly infinite lattice calculation that is performed by the lattice depletion codes. The initial flux, eigenvalue, and two adjoints as defined in reference [1] are solved and stored for future reference. The assemblies are then placed in a core as shown in a one-dimensional model given in Fig. 1. In this figure, γ is defined as the boundary current to flux ratio with the subscript indicating the interface. It is assumed that the core boundary conditions, which are notated as γ_{-1} and γ_2 in Fig. 1, are known beforehand.

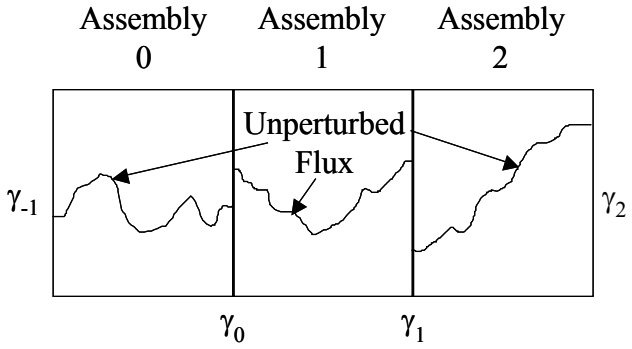

Figure 1. Example Core Layout

The eigenvalue for a given assembly, *i*, may be determined using boundary condition perturbation theory as the series

$$\lambda = \lambda_o + \varepsilon\lambda_1 + \varepsilon^2\lambda_2 \cdots + \varepsilon^n\lambda_n + O(\varepsilon^{n+1}) . \quad (1)$$

This series is dependant only on the initial state and the boundary current to flux ratios along the interface. Since there is only one fundamental eigenvalue for the core, the eigenvalue

computed for each assembly must be equal to this value and thus to each other. This allows for a system of equations to be defined in which the unknowns are the interface boundary current to flux ratios. Once these values are known, the entire core solution is known.

2.1 FIRST-ORDER CORE SOLUTION

If we truncate the eigenvalue series in Eq. (1) to the first order, we can state that the overall system eigenvalue is a constant for Fig. 1 as

$$\lambda_{0,0} + \lambda_{1,0} = \lambda_{0,1} + \lambda_{1,1} = \lambda_{0,2} + \lambda_{1,2} \tag{2}$$

where $\lambda_{l,i}$ represents the l^{th} perturbation order eigenvalue for assembly i. The first-order eigenvalue is found in reference 1 for assembly i as

$$\lambda_{1,i} = \frac{1}{N_i}\left[-\gamma_{i-1}\left\langle \overline{\varphi}^{*}_{0,i}\overline{\varphi}_{0,i} \right\rangle_{x_i^-} + \gamma_i \left\langle \overline{\varphi}^{*}_{0,i}\overline{\varphi}_{0,i} \right\rangle_{x_i^+} \right] \tag{3}$$

where

$$N_i = \left\langle \overline{\varphi}^{*}_{0,i} F_i \overline{\varphi}_{0,i} \right\rangle . \tag{4}$$

The brackets, $\langle \cdot \rangle$, represent phase space integration over the assembly. A subscript to this bracket implies a surface integration for the boundary indicated. The function $\overline{\varphi}_{0,i}$ is the phase space normalized flux, $\overline{\varphi}^{*}_{0,i}$ is the corresponding adjoint, F_i, is the fission operator, x_i^+ is the right side of the assembly, and x_i^- is the left side. The surface integration is broken up into two components in which the boundary to current flux ratio is constant along each interface. The negative sign in front of the left boundary current to flux ratio, γ_{i-1}, is due to the outward normal pointing in the negative x-direction. In addition, the left and right external surfaces are assumed be subject to the zero current boundary condition.

Now everything in Eq. (2) is known or can be computed except for the boundary current to flux ratios. In Fig. 1, Eq. (2) shows that two equations may be written for the two unknowns, γ_0 and γ_1. In a larger system, the unknown boundary current to flux ratios could also be solved with a linear system of equations in which the i^{th} equation is given as

$$\begin{aligned} &\lambda_{0,i} + \frac{1}{N_i}\left[-\gamma_{i-1}\left\langle \overline{\varphi}^{*}_{0,i}\overline{\varphi}_{0,i} \right\rangle_{x_i^-} + \gamma_i \left\langle \overline{\varphi}^{*}_{0,i}\overline{\varphi}_{0,i} \right\rangle_{x_i^+} \right] \\ &\quad = \lambda_{0,i+1} + \frac{1}{N_{i+1}}\left[-\gamma_{i}\left\langle \overline{\varphi}^{*}_{0,i+1}\overline{\varphi}_{0,i+1} \right\rangle_{x_{i+1}^-} + \gamma_{i+1} \left\langle \overline{\varphi}^{*}_{0,i+1}\overline{\varphi}_{0,i+1} \right\rangle_{x_{i+1}^+} \right] \end{aligned} . \tag{5}$$

2.2 SECOND-ORDER CORE SOLUTION

If we extend the eigenvalue solution to second-order in Eq. (2), then for an assembly the eigenvalue can be determined from the following set of equations:

$$\overline{\varphi}_{1,i} = \gamma_{i-1}\left\langle \Psi^*_{0,i}\overline{\varphi}_{0,i}\right\rangle_{x_i^-} - \gamma_i\left\langle \Psi^*_{0,i}\overline{\varphi}_{0,i}\right\rangle_{x_i^+} \tag{6}$$

$$\lambda_{2,i} = \frac{1}{N_i}\left[-\gamma_{i-1}\left\langle \overline{\varphi}^*_{0,i}\overline{\varphi}_{1,i}\right\rangle_{x_i^-} + \gamma_i\left\langle \overline{\varphi}^*_{0,i}\overline{\varphi}_{1,i}\right\rangle_{x_i^+} - \lambda_{1,i}\left\langle \overline{\varphi}^*_{0,i}F\overline{\varphi}_{1,i}\right\rangle\right] \tag{7}$$

The Green's function adjoint, $\Psi^*_{0,i}$, is a function of two-phase variables. Therefore an integration of this function returns a function of just one phase space. The second-order eigenvalue is determined by substitution of Eqs. (3) and (6) into Eq. (7). The resulting equations may be simplified by defining

$$\lambda_{1,i} = \gamma_{i-1}\hat{A}_{1,i} + \gamma_i\hat{B}_{1,i} \tag{8}$$

$$\overline{\varphi}_{1,i} = \gamma_{i-1}\hat{C}_{1,i}(x) + \gamma_i\hat{D}_{1,i}(x) \tag{9}$$

$$\lambda_{2,i} = \gamma^2_{i-1}\hat{A}_{2,i} + \gamma_{i-1}\gamma_i\hat{B}_{2,i} + \gamma^2_i\hat{C}_{2,i} \tag{10}$$

where the coefficients are given by

$$\hat{A}_{1,i} = -\frac{1}{N_i}\left\langle \overline{\varphi}^*_{0,i}\overline{\varphi}_{0,i}\right\rangle_{x_i^-} \tag{11}$$

$$\hat{B}_{1,i} = \frac{1}{N_i}\left\langle \overline{\varphi}^*_{0,i}\overline{\varphi}_{0,i}\right\rangle_{x_i^+} \tag{12}$$

$$\hat{C}_{1,i}(x) = \left\langle \Psi^*_{0,i}\overline{\varphi}_{0,i}\right\rangle_{x_i^-} \tag{13}$$

$$\hat{D}_{1,i}(x) = \left\langle \Psi^*_{0,i}\overline{\varphi}_{0,i}\right\rangle_{x_i^+} \tag{14}$$

$$\hat{A}_{2,i} = -\frac{1}{N_i}\left[\left\langle \overline{\varphi}^*_{0,i}\hat{C}_{1,i}(x)\right\rangle_{x_i^-} + \hat{A}_{1,i}\left\langle \overline{\varphi}^*_{0,i}F_i\hat{C}_{1,i}(x)\right\rangle\right] \tag{15}$$

$$\begin{aligned}\hat{B}_{2,i} = -\frac{1}{N_i}\Bigg[&\left\langle \overline{\varphi}^*_{0,i}\hat{D}_{1,i}(x)\right\rangle_{x_i^-} - \left\langle \overline{\varphi}^*_{0,i}\hat{C}_{1,i}(x)\right\rangle_{x_i^+} \\ &+ \hat{A}_{1,i}\left\langle \overline{\varphi}^*_{0,i}F_i\hat{D}_{1,i}(x)\right\rangle + \hat{B}_{1,i}\left\langle \overline{\varphi}^*_{0,i}F_i\hat{C}_{1,i}(x)\right\rangle\Bigg]\end{aligned} \tag{16}$$

$$\hat{C}_{2,i} = \frac{1}{N_i}\left[\left\langle \overline{\varphi}^*_{0,i}\hat{D}_{1,i}(x)\right\rangle_{x_i^+} - \hat{B}_{1,i}\left\langle \overline{\varphi}^*_{0,i}F_i\hat{D}_{1,i}(x)\right\rangle\right] \tag{17}$$

With the coefficients known from these equations, the eigenvalue for an assembly is easily determined as a quadratic polynomial. The i^{th} equation is given as

$$\begin{aligned}&\lambda_{0,i} + \hat{A}_{1,i}\gamma_{i-1} + \hat{B}_{1,i}\gamma_i + \hat{A}_{2,i}\gamma_{i-1}^2 + \hat{B}_{2,i}\gamma_{i-1}\gamma_i + \hat{C}_{2,i}\gamma_i^2 \\ &= \lambda_{0,i+1} + \hat{A}_{1,i+1}\gamma_i + \hat{B}_{1,i+1}\gamma_{i+1} + \hat{A}_{2,i+1}\gamma_i^2 + \hat{B}_{2,i+1}\gamma_i\gamma_{i+1} + \hat{C}_{2,i+1}\gamma_{i+1}^2\end{aligned} . \tag{18}$$

Not that this system of equations is nonlinear.

3. EXAMPLES

3.1 EXAMPLE 1:

Take two slabs of width 1 each with different material compositions as shown in Fig. 2. The boundary current-to-flux ratio, γ, changes sign for Assembly 1.

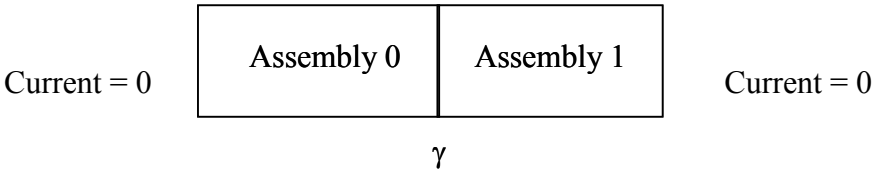

Figure 2. Sample Problem 1 Core Layout

We know that the analytical solution from reference [1] for a slab with infinite medium boundary conditions is

$$\Psi_0^* = \begin{cases} \dfrac{1}{2D}\left(x^2 + x_0^2\right) + \dfrac{1}{D}\left(\dfrac{1}{3} - x_0\right), & 0 \le x \le x_0 \\ \dfrac{1}{2D}\left(x^2 + x_0^2\right) + \dfrac{1}{D}\left(\dfrac{1}{3} - x\right), & x_0 \le x \le 1 \end{cases} \tag{19}$$

We also know the eigenvalue and the flux for any order. The first few (for a boundary condition perturbation at right side) are

$$\lambda_0 = \frac{\sigma_a}{\nu\sigma_f} \tag{20}$$

$$\overline{\varphi}_0 = \overline{\varphi}_0^* = 1 \tag{21}$$

$$\lambda_1 = \frac{\gamma}{\nu\sigma_f} \tag{22}$$

$$\overline{\varphi}_1 = \frac{\gamma}{2D}\left(\frac{1}{3} - x^2\right) \tag{23}$$

$$\lambda_2 = -\frac{\gamma^2}{3\nu\sigma_f D} \tag{24}$$

For a first order analysis we set the eigenvalues equal to each other:

$$\lambda_{0,0} + \lambda_{1,0} = \lambda_{0,1} + \lambda_{1,1} \tag{25}$$

or

$$\left(\frac{\sigma_a}{\nu\sigma_f}\right)_0 + \gamma\left(\frac{1}{\nu\sigma_f}\right)_0 = \left(\frac{\sigma_a}{\nu\sigma_f}\right)_1 - \gamma\left(\frac{1}{\nu\sigma_f}\right)_1 \tag{26}$$

which leads to a solution for γ as

$$\gamma = \left[\left(\frac{\sigma_a}{\nu\sigma_f}\right)_1 - \left(\frac{\sigma_a}{\nu\sigma_f}\right)_0\right] \Bigg/ \left[\left(\frac{1}{\nu\sigma_f}\right)_0 + \left(\frac{1}{\nu\sigma_f}\right)_1\right] \tag{27}$$

A second order solution is similar:

$$\lambda_{0,0} + \lambda_{1,0} + \lambda_{2,0} = \lambda_{0,1} + \lambda_{1,1} + \lambda_{2,1} \tag{28}$$

or

$$\begin{aligned}\left(\frac{\sigma_a}{\nu\sigma_f}\right)_0 + \gamma\left(\frac{1}{\nu\sigma_f}\right)_0 - \gamma^2\left(\frac{1}{3\nu\sigma_f D}\right)_0 \\ = \left(\frac{\sigma_a}{\nu\sigma_f}\right)_1 - \gamma\left(\frac{1}{\nu\sigma_f}\right)_1 - \gamma^2\left(\frac{1}{3\nu\sigma_f D}\right)_1\end{aligned} \tag{29}$$

which is a quadratic equation in γ.

Now let's take a sample case with the parameters given in Table I. These values were chosen to demonstrate the importance of higher-order methods and do not reflect any realistic case. The exact eigenvalue solution as determined from a fine-mesh diffusion code is 0.4696. The first order solution starts by solving Eq. (27) to get a γ of 0.5. Plugging this into Eq. (26) for the left hand side gives an eigenvalue of 0.5 (6.5% error). The second order solution is similar but Eq. (29) is solved. Using the positive root results in a γ of 0.4807, which gives an eigenvalue from Eq. (29) of 0.4679 (0.4% error).

Table I. Sample Problem 1 Parameters

	Assembly 1	Assembly 2
D	1	1.5
σ_a	1	1
$\nu\sigma_f$	3	1

A code was developed to numerically implement the methods presented in this paper up to second order. The eigenvalue and flux are computed and compared to the exact solution. The results are shown in Table II with the flux RMS % defined as

$$\text{Flux RMS}\,\% = \left[\frac{1}{N-1} \sum_{i=1}^{N} \left[\left(y_{exact,i} - y_{computed,i} \right) / y_{exact,i} \right]^2 \right]^{1/2} . \tag{30}$$

Table II. Sample Problem 1 Results

	Eigenvalue	Error %	Flux RMS %
Exact	0.470	---	---
1st Order	0.500	6.5%	1.6%
2nd Order	0.468	0.4%	0.2%

The numerical and analytical solutions agree for the eigenvalue in Table II. The second-order results represent a significant increase in accuracy. The graph of the flux is shown in Fig. 3. As seen from this figure, excellent agreement in the flux is obtained with the second-order method.

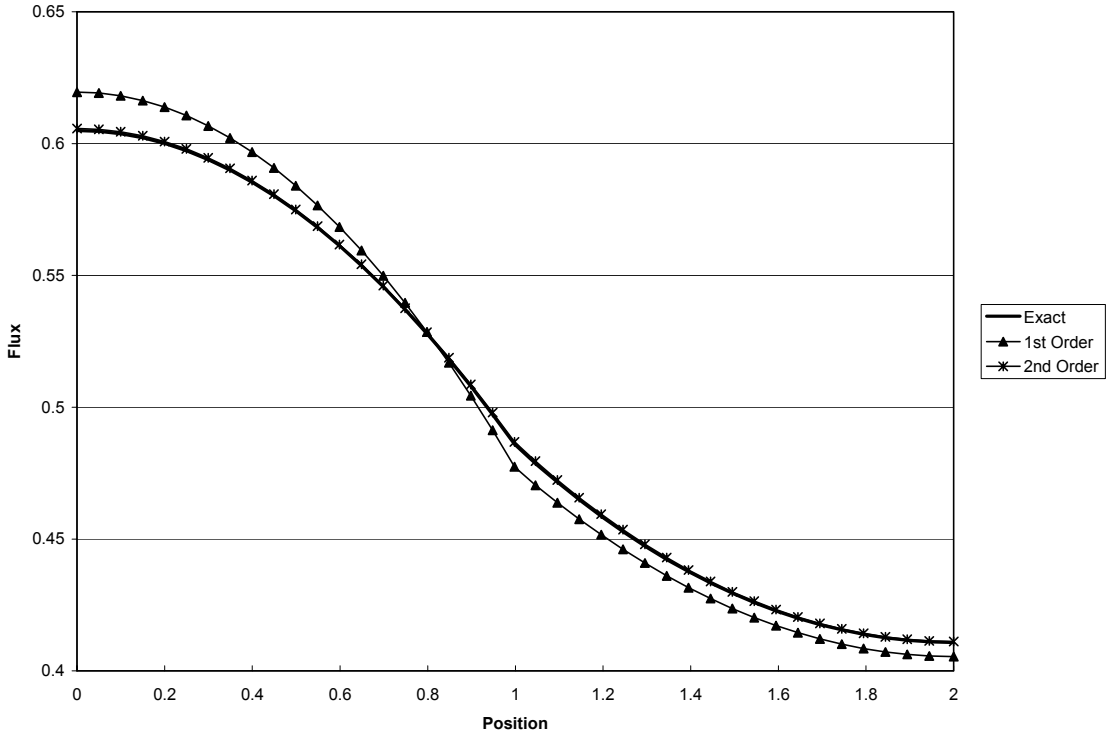

Figure 3. Sample Problem 1 Flux

3.2 EXAMPLE 2

This example follows from the previous example with the addition of modifying the external boundary condition by allowing for some leakage of neutrons through the external boundaries. Each external boundary experiences the same change in albedo from the initial boundary condition of zero current. In such a case, the interface current to flux ratio γ may be solved in a quadratic equation similar to Eq. (29):

$$\left(\frac{\sigma_a}{\nu\sigma_f}\right)_0 + (\gamma - \gamma_b)\left(\frac{1}{\nu\sigma_f}\right)_0 - (\gamma^2 - \gamma_b^2)\left(\frac{1}{3\nu\sigma_f D}\right)_0 = \left(\frac{\sigma_a}{\nu\sigma_f}\right)_1 - (\gamma + \gamma_b)\left(\frac{1}{\nu\sigma_f}\right)_1 - (\gamma^2 + \gamma_b^2)\left(\frac{1}{3\nu\sigma_f D}\right)_1 \quad (31)$$

where γ_b is the external boundary current to flux ratio.

Using a fine-mesh test code to determine the exact eigenvalue, λ_{Exact}, and solving the above equation, the following results were obtained:

Table III. Sample Problem 2 Results

γ_b	$\gamma_{Computed}$	$\lambda_{Computed}$	λ_{Exact}	% Error
-0.9	0.826	0.743	0.899	17.41
-0.7	0.761	0.702	0.804	12.74
-0.5	0.690	0.649	0.708	8.36
-0.3	0.611	0.586	0.613	4.46
-0.1	0.526	0.510	0.517	1.41
-0.01	0.485	0.472	0.474	0.47
0.0	0.481	0.468	0.470	0.36
0.01	0.476	0.464	0.465	0.31
0.1	0.434	0.423	0.422	-0.13
0.3	0.333	0.322	0.326	1.33
0.5	0.225	0.208	0.231	9.80
0.7	0.108	0.080	0.135	40.66
0.8	0.046	0.011	0.088	87.65
0.85	0.015	-0.025	0.064	139.85

This result shows an additional perturbation on top of the underlying perturbation theory used to solve for the boundary interface condition. As γ_b changes from 0.0 on the above table, the percent error grows. For negative γ_b, the error grows slow but steady. However, for the case of increasing γ_b, which represents neutron multiplication outside the system, the error grows extremely large after 0.5. By the time it is at 0.85, the computed eigenvalue has reached a negative and physically impossible value. In order to model such cases, a higher order boundary condition perturbation theory could be used. Another approach is computing a new initial condition and adjusting the perturbation equations from reference [1] so they no longer assume an infinite medium approximation.

CONCLUSIONS

In this paper, we developed a coarse-mesh response matrix method based on high-order boundary condition perturbation theory that solves for the interface current-to-flux ratios for an entire core as the solution to a system of linear or nonlinear equations in diffusion theory. Knowing the current-to-flux ratios, one may then use the high-order boundary condition perturbation theory of reference [1] to solve for the flux and eigenvalue.

The regular and the Green's function adjoint must be solved for each unique assembly type in the core. While the indexing in the paper was based on assembly, all precomputed values such as initial flux, adjoints, and initial eigenvalue are based on the unique assemblies used in the core. Also, the coefficients of the eigenvalue and flux, as given in Eqs. (11) - (17), are needed for the unique assembly types only. This greatly reduces storage requirements.

The first-order method is very fast since it only involves a linear solution based on the regular adjoint, $\overline{\varphi}_0^*$. The Green's function is only needed if the first-order flux is desired. This represents a quick solution where the first-order approximations are accurate enough. This method may also prove to be a good initial seed for the eigenvalue and flux for other methods that require a good initial guess.

Two example problems were used to test the accuracy of the method presented in this paper. The first example was a very simple two region case where the adjoints where known analytically. The numerical solution was compared to the analytical solution to verify the correctness of the method. The accuracy of the method was further tested for the same problem with a non-reflective boundary condition. The results showed that a higher order analysis was needed to achieve high accuracy for large boundary current to flux ratios (large perturbations from the infinite lattice case).

There are many avenues of future activity stemming forth from this work. An obvious extension would be to continue this work beyond the second-order theory. This could lead to an analysis of error, precomputation time, computation time, rate of convergence, storage requirements, etc. for each additional order of perturbation to see the potential benefits of high order analysis.

The Achilles' heel of this method is in the computation of the Green's function adjoint, Ψ_0^*. The numerical solution requires for the diffusion equation to be solved for each point in phase space. Not only does this lead to a large precomputation time, it also affects the accuracy in which this adjoint may be solved. High order perturbation methods will see little additional advantage without a more accurate solution to this adjoint.

Finally, this work could be extended to transport theory. Although, the concept should be the same, the functions and solution methods may be much more complex. Previous work in high-order boundary condition perturbation methods for transport theory [3] show distinct advantages in the accuracy gained.

REFERENCES

1. M. S. McKinley and F. Rahnema, "Higher-Order Boundary Condition Perturbation Theory for the Diffusion Approximation", *Nucl. Sci. Eng.*, **136**, 15 (Sept. 2000)..

2. Rahnema, F., McKinley, M. S., 2001. "Higher-Order Cross Section Homogenization Method," *Ann. Nucl. Energy*, **29**, 875 (2002).

3. M. S. McKinley and F. Rahnema, "High-Order Boundary Condition Perturbation Theory for the Neutron Transport Equation," *Nucl. Sci. Eng.,* **140**, 3 (Mar. 2002).